Cellular and Molecular Neurobiology (2020) 40:153–166
https://doi.org/10.1007/s10571-019-00732-1

ORIGINAL RESEARCH

Bcl-2 Overexpression Induces Neurite Outgrowth via the Bmp4/Tbx3/NeuroD1 Cascade in H19-7 Cells

Yun Young Lee[1,2] · Hye-jin Choi[2] · So Young Lee[1] · Shin-Young Park[2] · Min-Jeong Kang[1] · Jinil Han[1,3] · Joong-Soo Han[1,2]

Received: 16 April 2019 / Accepted: 29 August 2019 / Published online: 6 September 2019

Abstract

Bcl-2 is overexpressed in the nervous system during neural development and plays an important role in modulating cell survival. In addition to its anti-apoptotic function, it has been suggested previously that Bcl-2 might act as a mediator of neuronal differentiation. However, the mechanism by which Bcl-2 might influence neurogenesis is not sufficiently understood. In this study, we aimed to determine the non-apoptotic functions of Bcl-2 during neuronal differentiation. First, we used microarrays to analyze the whole-genome expression patterns of rat neural stem cells overexpressing *Bcl-2* and found that *Bcl-2* overexpression induced the expression of various neurogenic genes. Moreover, *Bcl-2* overexpression increased the neurite length as well as expression of *Bmp4*, *Tbx3*, and proneural basic helix–loop–helix genes, such as *NeuroD1*, *NeuroD2*, and *Mash1,* in H19-7 rat hippocampal precursor cells. To determine the hierarchy of these molecules, we selectively depleted *Bmp4*, *Tbx3*, and *NeuroD1* in *Bcl-2*-overexpressing cells. *Bmp4* depletion suppressed the upregulation of Tbx3 and NeuroD1 as well as neurite outgrowth, which was induced by *Bcl-2* overexpression. Although *Tbx3* knockdown repressed Bcl-2-mediated neurite elaboration and downregulated NeuroD1 expression, it did not affect *Bcl-2*-induced Bmp4 expression. While the depletion of *NeuroD1* had no effect on the expression of Bcl-2, Bmp4, or Tbx3, Bcl-2-mediated neurite outgrowth was suppressed. Taken together, these results demonstrate that Bcl-2 regulates neurite outgrowth through the Bmp4/Tbx3/NeuroD1 cascade in H19-7 cells, indicating that Bcl-2 may have a direct role in neuronal development in addition to its well-known anti-apoptotic function in response to environmental insults.

Keywords Bcl-2 · Neurite outgrowth · Bmp4 · Tbx3 · NeuroD1

Abbreviations

NPCs	Neural precursor cells
bHLH	Basic helix–loop–helix
CNS	Central nervous system
bFGF	Basic fibroblast growth factor

Introduction

Bcl-2 gene was identified at the breakpoint of the t(14;18)(q32;q21) chromosomal translocation that is associated with human follicular lymphoma, and since then, it has been shown that the Bcl-2 protein is mainly located on the mitochondrial outer membrane and is responsible for the regulation of programmed cell death (Pegoraro et al. 1984; Hockenbery et al. 1990). Currently, it is recognized that Bcl-2 can not only modulate apoptosis by interacting with other pro- or anti-apoptotic Bcl-2 family members, but it also has an anti-autophagy function by directly binding

Electronic supplementary material The online version of this article (https://doi.org/10.1007/s10571-019-00732-1) contains supplementary material, which is available to authorized users.

Yun Young Lee and Hye-jin Choi have contributed equally to this work.

✉ Joong-Soo Han
jshan@hanyang.ac.kr

[1] Department of Biomedical Sciences, Graduate School of Biomedical Science and Engineering, Hanyang University, Seoul 04763, Republic of Korea

[2] Biomedical Research Institute and Department of Biochemistry and Molecular Biology, College of Medicine, Hanyang University, Seoul 04763, Republic of Korea

[3] Gencurix, Inc, Hanwha Bizmetro 1, Guro 3-dong, Guro-gu, Seoul 08394, Republic of Korea

with Beclin-1 (Adams and Cory 1998; Pattingre et al. 2005). Consequently, Bcl-2 is considered to be a arbiter of cell survival for development, tissue homeostasis, protection against diverse insults, and various diseases including cancer (Adams and Cory 1998).

In mice, Bcl-2 is highly expressed in the organs related to the immune system (such as the thymus and the spleen) and the brain (Hockenbery et al. 1991; Abedohmae et al. 1993). During brain development, the mRNA levels of *Bcl-2* are the highest on embryonic day 15, which is the stage of neurogenesis, indicating that Bcl-2 may have a considerable impact on the process of neuronal development in the CNS (central nervous system) (Abedohmae et al. 1993; Merry et al. 1994). According to previous reports, overexpression of *Bcl-2* prevents neurotrophic factor deprivation-induced neuronal apoptosis in embryonic neurons (Allsopp et al. 1993). Moreover, *Bcl-2* transgenic mice are protected against middle cerebral artery occlusion-induced ischemia (Martinou et al. 1994), and *Bcl-2*-deficient mice exhibit progressive degeneration of motor, sympathetic, and sensory neurons during early postnatal development (Michaelidis et al. 1996). In addition to these neuroprotective functions, Bcl-2 has also been shown to influence neurogenesis in pheochromocytoma and neuroblastoma cell lines (Sato et al. 1994; Hanada et al. 1993). Zhang et al. (1996) reported that Bcl-2 directly modulated neuronal differentiation in human neural crest cells, and Hilton et al. (1997) suggested that Bcl-2 had an impact on the axonal growth rate of the embryonic sensory neurons. Moreover, Bcl-2 promotes regeneration of injured axons in the mammalian CNS (Chen et al. 1997), indicating that Bcl-2 may have a direct function on neurogenesis in addition to its well-documented role as a suppressor of apoptosis. Nevertheless, the precise non-apoptotic functions of Bcl-2 during neuronal differentiation still remain unclear.

Neurogenesis is the differentiation process for neuronal lineage commitment of multipotent neural stem cells either during the development of the fetal nervous system or during the regeneration of an impaired adult nervous system, which is spatiotemporally coordinated by a variety of intrinsic and extrinsic factors in stem cell niches (Gage 2000; Paridaen and Huttner 2014). Proneural bHLH proteins, including NeuroDs and neurogenins, are essential transcriptional regulators for cell fate specification in neural stem cell niches (Paridaen and Huttner 2014; Ross et al. 2003). Moreover, deregulated expression or mutation of the bHLH genes occurs in brain cancers, as well as neurodevelopmental, neuropsychiatric, and neurodegenerative disorders (Dennis et al. 2019). Their expression is also regulated by various signaling networks such as Notch, Wnt, and BMP (Dennis et al. 2019). However, the signaling pathway that couples Bcl-2 to the regulation of bHLH transcription factors during neuronal differentiation is not yet fully understood.

Here, we aimed to clarify the non-apoptotic functions of Bcl-2 during neuronal differentiation and to explain the mechanism by which Bcl-2 regulates neurite formation. Using gain- or loss-of-function studies, we showed that the neurite lengths of differentiating H19-7 cells were affected by the modulation of the *Bcl-2* gene. Moreover, we observed that *Bcl-2* overexpression influenced various neurogenic factors by analyzing whole-genome expression patterns obtained through microarrays. In conclusion, we demonstrated that *Bcl-2* overexpression promoted neurite outgrowth through the Bmp4/Tbx3/NeuroD1 cascade in the H19-7 cells, indicating that Bcl-2 may have a direct role in neuronal development in addition to its well-known anti-apoptotic function.

Materials and Methods

Materials

The cell culture materials, such as Dulbecco's modified Eagle's medium (DMEM) with L-glutamine and low glucose, fetal bovine serum (FBS), phosphate-buffered saline (PBS), penicillin/streptomycin, and trypsin/EDTA, were purchased from WISENT (St. Bruno, QC, Canada). G-418 was obtained from Duchefa (Haarlem, Netherlands). RNAiso Plus for RNA extraction was purchased from Takara Bio (Otsu, Japan), Reverse Transcription Master Mix for cDNA synthesis was obtained from Elpis Bio (Daejeon, Korea), and Go*Taq*® DNA polymerase kits were purchased from Promega (Madison, WI, USA). SensiFAST™ SYBR® No-ROX kits were purchased from Bioline (London, UK). The antibodies used were purchased as follows: Bcl-2 (SC-7382) from Santa Cruz Biotechnology (Santa Cruz, CA, USA), Calnexin (ADI-SPA-860) from Enzo Life Sciences (Farmingdale, NY, USA); Bmp4 (ab39973), Tbx3(ab99302), and NeuroD1 (ab16508) from Abcam (Cambridge, UK); GFP (11814460001) from Roche (Indianapolis, IN, USA), β-tubulin type III (TUJ1, 802001) from BioLegend (San Diego, CA, USA), Alexa Flour® 488-conjugated goat anti-rabbit IgG (A11008) from Thermo Fisher Scientific (Rockford, IL, USA), and Cy™ 3-conjugated AffiniPure goat anti-rabbit IgG (H + L) (111-165-144) from Jackson ImmunoResearch (West Grove, PA, USA). All other chemicals were of analytical grade.

Cell Culture

H19-7 cells, which are conditionally immortalized rat hippocampal precursor cells with a temperature-sensitive SV40 large T antigen, were maintained in DMEM supplemented with 10% (v/v) heat-inactivated FBS, 100 units/mL penicillin, and 100 μg/mL streptomycin under 0.2 mg/mL G-418

selection at 33 °C (the temperature at which the SV40 large T antigen is functional) in a humidified incubator with 5% CO_2. To induce differentiation, the medium was changed to N2 medium supplemented with 20 ng/mL bFGF (R&D Systems, Minneapolis, MN, USA), and the cells were incubated at 39 °C for 2 days. Neural precursor cells (NPCs) were obtained from pregnant Sprague–Dawley rats. Protocols were reviewed and approved by the Institutional Animal Care and Use Committee of Hanyang Laboratory Animal Research Center (2014-0126A). The embryonic brain cortices from E14 rat embryos were mechanically triturated in a Ca^{2+}/Mg^{2+}-free Hank's balanced salt solution (HBSS; Gibco, Grand Island, NY, USA), seeded at 2×10^5 cells in 100-mm culture dishes (Corning Life Sciences, Acton, MA, USA), pre-coated with 15 μg/mL poly-L-ornithine (Sigma-Aldrich, St. Louis, MO, USA) and 1 μg/mL fibronectin (Invitrogen, Carlsbad, MO, USA), and cultured for 5 to 6 days in N2 medium supplemented with bFGF. The cell clusters generated were dissociated in HBSS, plated on fresh culture dishes, and induced for additional proliferation in N2 + bFGF up to 70 to 80% cell confluency before the cells were subjected to differentiation for 2 days.

Gene Expression Profiling Using cDNA Microarrays

Microarray analysis was performed using tools from the commercial microarray service Ebiogen (Seoul, Korea) and deposited in the NCBI Gene Expression Omnibus (GEO, http://www.ncbi.nlm.nih.gov/geo) repository (accession number GSE130481). In brief, the gene expression profiles of rat NPCs from the vector + bFGF group (proliferation control), the vector − bFGF group (differentiation control), and the *Bcl-2* + bFGF group (*Bcl-2* overexpression) were compared using cDNA microarrays. NPCs derived from the E14 rat embryos were transiently transfected with 4 μg of either MSCV-IRES-EGFP or *rBcl-2*-MSCV-IRES-EGFP using a Nucleofector™ kit (Lonza, Walkersville, MD, USA) according to the manufacturer's protocol. Total RNA was then isolated and amplified. The amplified cRNA was hybridized to an Agilent Rat Oligo Microarray (44 K) (Agilent Technology, Palo Alto, CA, USA) at 65 °C for 17 h in an Agilent DNA microarray hybridization oven and then washed. The hybridized images were scanned using an Agilent DNA microarray scanner and quantified using Feature Extraction software (Agilent Technology). The data normalization and selection of the genes that had undergone fold changes were performed using GeneSpring GX software, version 7.3 (Agilent Technology). The gene classification was performed using BioCarta (http://www.biocarta.com), GenMAPP (http://www.genmapp.org), and DAVID (http://david.abcc.ncifcrf.gov). To obtain insights into the biological processes related with neural development, Gene Ontology (GO) analysis was performed. Using GO terms corresponding to 'nervous system development,' the neural development-related genes were selected for further analysis. All microarray analyses and visualization were conducted using R software, version 3.4.1 (www.r-project.org).

Retroviral Construction and Infection

Rat *Bcl-2* cDNA was amplified from NPCs of E14 Sprague–Dawley rat embryos using PCR and cloned into the retroviral vector MSCV-IRES-EGFP. The construct was obtained using a forward primer containing a BglII site (5′-GAAGATCTATGGCGCAAGCCGGGAGA-3′) and a reverse primer containing an EcoRI site (5′-GGAATT CTCACTTGTGGCCCAGGTATGCAC-3′). PCR mixtures contained 1 μL of cDNA from NPCs, 5 μL of 10X PCR buffer, 5 μL of dNTP mix (2.5 mM), 1 μL of Taq polymerase (10 units/μL, Pyrobest, Takara Bio) adjusted to 50 μL with distilled water. The PCR amplification consisted of denaturation for 5 min at 95 °C followed by 30 cycles of 30 s at 95 °C, 30 s at 60 °C, and 90 s at 72 °C, with a final extension for 7 min at 72 °C. The PCR product was separated via electrophoresis on a 1.5% agarose gel and visualized using a 3UV™ transilluminator (UVP, Upland, CA, USA). The DNA band of the expected size was excised, purified using a FavorPrep™ GEL/PCR purification mini kit (Favorgen Biotech, Pingtung, Taiwan), and digested with the appropriate restriction enzymes (BglII and EcoRI; New England Biolabs, Beverly, MA, USA) at 37 °C. The digested sample was then ligated into the MSCV-IRES-EGFP retroviral vector. The cloned rat *Bcl-2* was confirmed using sequencing (Cosmo Genetech, Seoul, Korea), and the sequence was aligned with the NCBI rat *Bcl-2* mRNA sequence (NM_016993.1) using the Genomatix pairwise comparison program (http://www.genomatix.de/cgi-bin/dialign/dialign.pl). The viral particles were produced by transfecting the retrovirus packaging cell line 293GPG with the cloned vector using polyethylenimine (PEI; Sigma-Aldrich), and supernatants containing viral particles were harvested after incubation for 48 h. For viral infection, H19-7 cells were incubated with a viral suspension (4×10^6 particles/mL) containing polybrene (1 μg/mL; Sigma-Aldrich) for 4 h followed by transfer to fresh medium.

Transient Transfection with Small Interfering RNAs

Bcl-2, *Bmp4*, *Tbx3*, and *NeuroD1* siRNAs, as well as control siRNA (Bioneer, Daejeon, Korea), were transiently transfected into H19-7 cells for loss-of-function studies. The siRNA sequences were as follows: *Bcl-2* (5′-GAAUCA AGUGUUCGUCAUA-3′ and 5′-UAUGACGAACACUUG AUUC-3′), *Bmp4* (5′-GACUACUGGACACCAGACU-3′ and 5′-AGUCUGGUGUCCAGUAGUC-3′), *Tbx3* (5′-CUG GAUAAAAAGGCCAAGU-3′ and 5′-ACUUGGCCUUUU

UAUCCAG-3′), and *NeuroD1* (5′-GAAACAUGACCAAAU CAUA-3′ and 5′-UAUGAUUUGGUCAUGUUUC-3′). Each siRNA (100 nM) was introduced into the cells using PEI transfection reagent.

Immunostaining and Measurement of Neurite Outgrowth

Cells were washed with PBS and fixed with 4% (w/v) paraformaldehyde (PFA; Sigma-Aldrich) for 15 min followed by washing three times with 0.1% bovine serum albumin (BSA; Sigma-Aldrich) in PBS at 25 °C. The cells were permeabilized with 0.3% Triton X-100 in PBS for 20 min and blocked with 10% normal goat serum in PBS for 1 h at room temperature. Next, the cells were incubated with anti-TUJ1 antibody (1:2000) and anti-GFP antibody (1:500) at 4 °C followed by incubation with Cy™ 3-conjugated AffiniPure goat anti-rabbit IgG (H + L) (1:200) and Alexa Flour® 488-conjugated goat anti-rabbit IgG (1:500) for 1 h before mounting with Vectashield (Vector Laboratories, Burlingame, CA, USA) containing 4, 6-diamidino-2-phenylindone (DAPI). The immunoreacted cells were imaged using a fluorescence microscope (Leica Microsystems, Wetzlar, Germany), and the morphological characteristics were quantified using ImageJ software (NIH; http://rsb.Info.nih.gov/ij/). The neurite length was defined as the distance from the soma to the tip of the branch. The neurite length data were obtained from ten randomly selected areas from at least three independent experiments, and more than 100 cells were counted for each group in each experiment.

Reverse Transcription (RT)-PCR and Real-Time PCR

Total RNA was isolated using RNAiso Plus according to the manufacturer's protocol. Next, 1 μg of isolated total RNA was incubated with Reverse Transcription Master Premix kit for 60 min at 37 °C. The cDNA was mixed with specific primers and Go*Taq*® DNA polymerase, and the mixtures were amplified using a thermocycler (Takara Bio). The primer sequences used were as follows: *Bcl-2* (5′-CCTGGC ATCTTCTCCTTCCA-3′ and 5′-CACCCCATCCCTGAA GAGTT-3′), *Gapdh* (5′-GGCATTGCTCTCAATGACAA-3′ and 5′-AGGGCCTCTCTCTTGCTCTC-3′), *Bmp4* (5′-GAG ATCGCCACCTACAGGAA-3′ and 5′-GCTCCTGCTTCG ACTCCTTA-3′), *Tbx3* (5′-TTTGGCCATGTCGCCTTT TG-3′ and 5′-GAGCGGCTATTCAGTTCCGA-3′), *NeuroD1* (5′-CTCAGTTCTCAGGACGAGGA-3′ and 5′-TAG TTCTTGGCCAAGCGCAG-3′), *NeuroD2* (5′-TTCTCG CTCAAGCAGGACTC-3′ and 5′-GCGTTGAGCTCCTCG TACAT-3′), *Mash1* (5′-GGCTCAACTTCAGTGGCTTC-3′ and 5′-TGGAGTAGTTGGGGGAGATG-3′). The PCR conditions were as follows: denaturation at 95 °C for 30 s, annealing at 60 °C (*NeuroD1*, 58 °C) for 30 s, and extension at 72 °C for 40 s (*Bcl-2*, 28 cycles; *Gapdh*, 25 cycles; *Bmp4*, *Tbx3*, *NeuroD1*, *NeuroD2*, and *Mash1*, 33 cycles). The PCR products were analyzed on a 1.5% agarose gel. For real-time PCR, 1 μL of cDNA was amplified in duplicate in a final volume of 20 μL using the SensiFAST™ SYBR NO-ROX® kit and the RT-PCR primers listed above. Thermocycling conditions were 95 °C for 10 min followed by 40 cycles of 95 °C for 15 s and 58 °C (*NeuroD1*) or 60 °C (all other genes) for 1 min. The primer sequences for real-time PCR were the same as for RT-PCR.

Western Blot Analysis

Protein expression was analyzed by immunoblotting as described previously (Zhang et al. 2019; Pan et al. 2017). The cells were lysed in 20 mM Tris/HCl at pH 7.5 with 150 mM NaCl, 1 mM EDTA, 1 mM EGTA, 2.5 mM sodium pyrophosphate, 1% Triton X-100, and 1 mM PMSF. Samples containing 30 μg of total protein were loaded onto 12% SDS-PAGE gels, electrophoresed, and transferred onto nitrocellulose membranes (Amersham Biosciences, Piscataway, NJ, USA). After blocking with 5% nonfat dried milk for 1 h, the membranes were incubated with primary antibodies followed by a horseradish peroxidase (HRP)-conjugated secondary antibody (1:2000; Jackson ImmunoResearch). Specific bands were detected using enhanced chemiluminescence (ECL) (Thermo Fisher Scientific), and band intensities were quantified using ImageJ software.

Statistical Analysis

Statistical analysis was performed with SPSS software, version 18.0 (SPSS Inc., Chicago, IL, USA). The data were expressed as the mean ± SD of at least three independent experiments. Comparisons between groups were made using the unpaired Student's *t* test. p values < 0.05 were considered statistically significant.

Results

Bcl-2 Affects Neuronal Differentiation of Rat Hippocampal Progenitor Cells

We previously reported that phospholipase D1 (PLD1), a membrane-anchored enzyme that hydrolyzes phosphatidylcholine into phosphatidic acid, which acts as a lipid second messenger, and the polar head group choline (Park and Han 2018), increases Bcl-2 expression via the PLA2/Cox2/EP4/PKA/p38MAPK/CREB cascade in rat NPCs and via the JNK/STAT3 pathway in rat hippocampal progenitor cells during neuronal differentiation (Park et al. 2014; Yoon et al. 2012). Next, we sought to determine

how Bcl-2 influences the process of neuronal differentiation. To investigate whether the modulation of *Bcl-2* impacts neurite outgrowth, control or *Bcl-2* siRNA was transfected into H19-7 cells and then stimulated using N2 medium supplemented with 20 ng/mL bFGF for neuronal differentiation. As shown in Fig. 1a and b, bFGF-induced neurite outgrowth was repressed by *Bcl-2* depletion compared to the bFGF-treated control siRNA group. Inversely, *Bcl-2* was overexpressed through retroviral transduction with MSCV-IRES-EGFP or *rBcl*-2-MSCV-IRES-EGFP followed by stimulation with bFGF. As shown in Fig. 1c and d, the neurite length of GFP^+ cells was significantly potentiated compared with the bFGF-treated vector group. Moreover, these phenomena could be completely reproduced in E14 rat cortical NPCs (Fig. S1). These results suggest that Bcl-2 might be directly involved in neuronal differentiation.

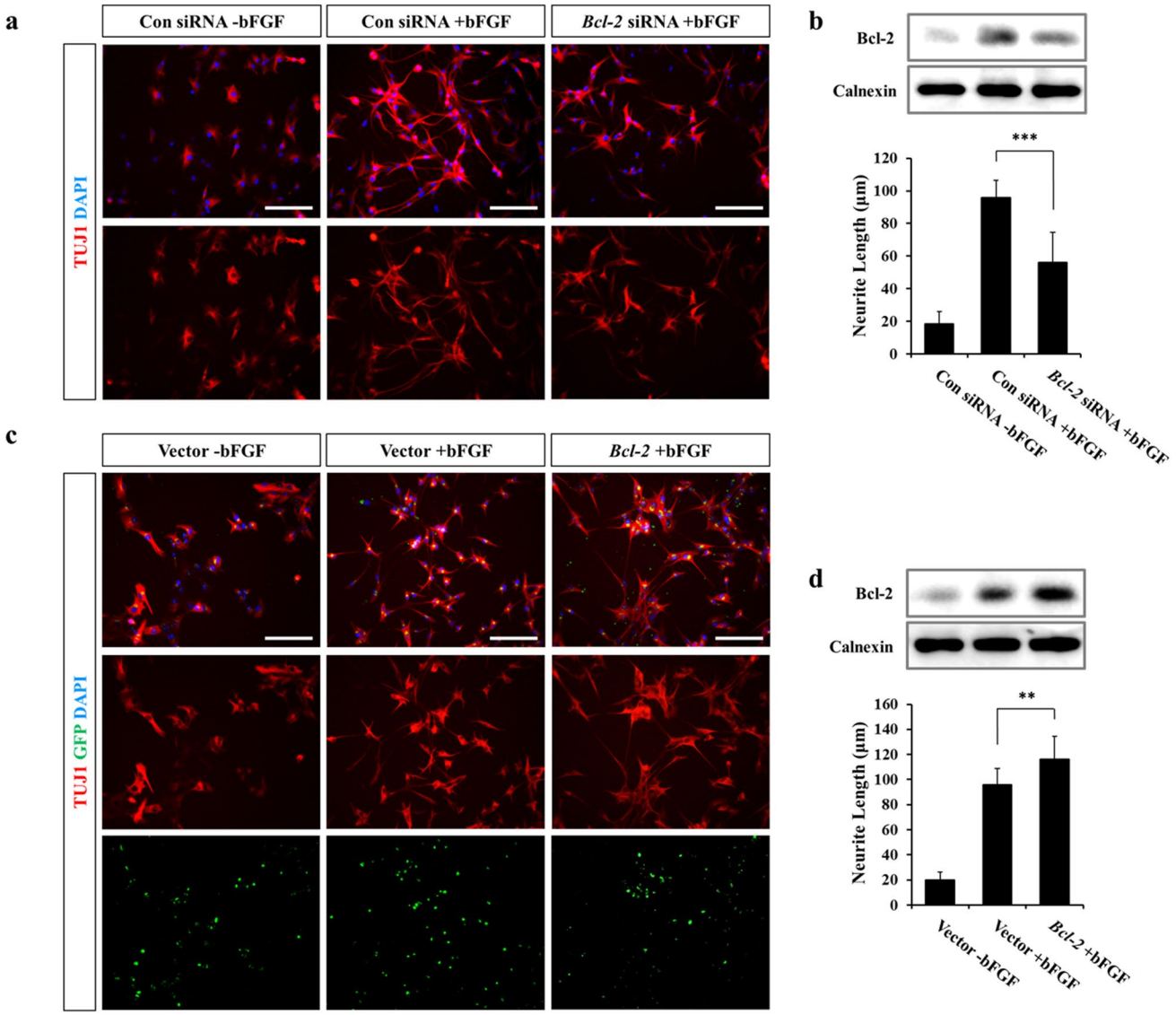

Fig. 1 Effect of *Bcl-2* gene modulation during neuronal differentiation in H19-7 cells. **a** H19-7 cells were transfected with control or *Bcl-2* siRNA for 2 days, after which the medium was changed to N2 medium supplemented with 20 ng/mL bFGF and the temperature shifted to 39 °C for 2 days. The cells were immunostained with TUJ1. Scale bar, 100 μm. **b** Immunoblotting was performed to verify the knockdown efficiency, and the neurite lengths of the $TUJ1^+$ cells were measured from 10 randomly selected areas from at least three independent experiments and presented as the mean ± SD. ***$p < 0.001$. **c** MSCV-IRES-EGFP or *rBcl*-2-MSCV-IRES-EGFP vectors were introduced into the cells through retroviral transduction for 2 days, followed by stimulation with bFGF and shifting the temperature to 39 °C for 2 days. **d** Cells were then immunostained with TUJ1 and GFP. Scale bar, 100 μm. The results are presented as the mean ± SD of three independent experiments. **$p < 0.01$

Bcl-2 Overexpression Increases Expression of Various Neurogenic Factors in NPCs

To investigate whether *Bcl-2* overexpression regulates the expression of neurogenic factors, we examined the gene expression patterns of NPCs derived from the cerebral cortex of E14 rat embryos by using microarrays. We found that the expression of 4762 genes was upregulated by *Bcl-2* overexpression, and of these, 3537 genes overlapped with the genes upregulated by the differentiation stimuli (Fig. 2a). On the other hand, out of the 6116 genes that were decreased by *Bcl-2* overexpression, 4989 of them overlapped with the genes downregulated by differentiation stimulation (Fig. S2). Additionally, 706 genes were identified as genes involved in the nervous system development through GO term analysis (Fig. 2b). Among them, *Bcl-2* overexpression upregulated 372 genes and downregulated 334 genes (Table S1). As in the differentiated control group (− bFGF), a variety of neurogenic marker genes, such as *Map2*, *Mapt*, *Synj1*, and *Snap25*, were increased by *Bcl-2* overexpression (Fig. 2b). Moreover, neurogenic bHLH transcription factors, including *NeuroD2* and *Ascl1* (*Mash1*), as well as *Bmp4* and *Tbx3* were increased by *Bcl-2* overexpression (Fig. 2b). Next, we verified whether the microarray results could be reproduced in H19-7 cells. As shown in Fig. 3a and b, *Bcl-2* overexpression induced a significant increase in neurite outgrowth. Moreover, the genes identified in the microarrays (*Bmp4*, *Tbx3*, *NeuoD1*, *NeuroD2*, and *Mash1*) showed significantly increased mRNA levels (Fig. 3c, d). The expression of the Bmp4, Tbx3, and NeuroD1 proteins also showed a similar tendency (Fig. 3e, f). In summary, *Bcl-2* overexpression upregulates the expression of various neurogenic factors, such as Bmp4, Tbx3, and NeuroD1, and increases neurite outgrowth.

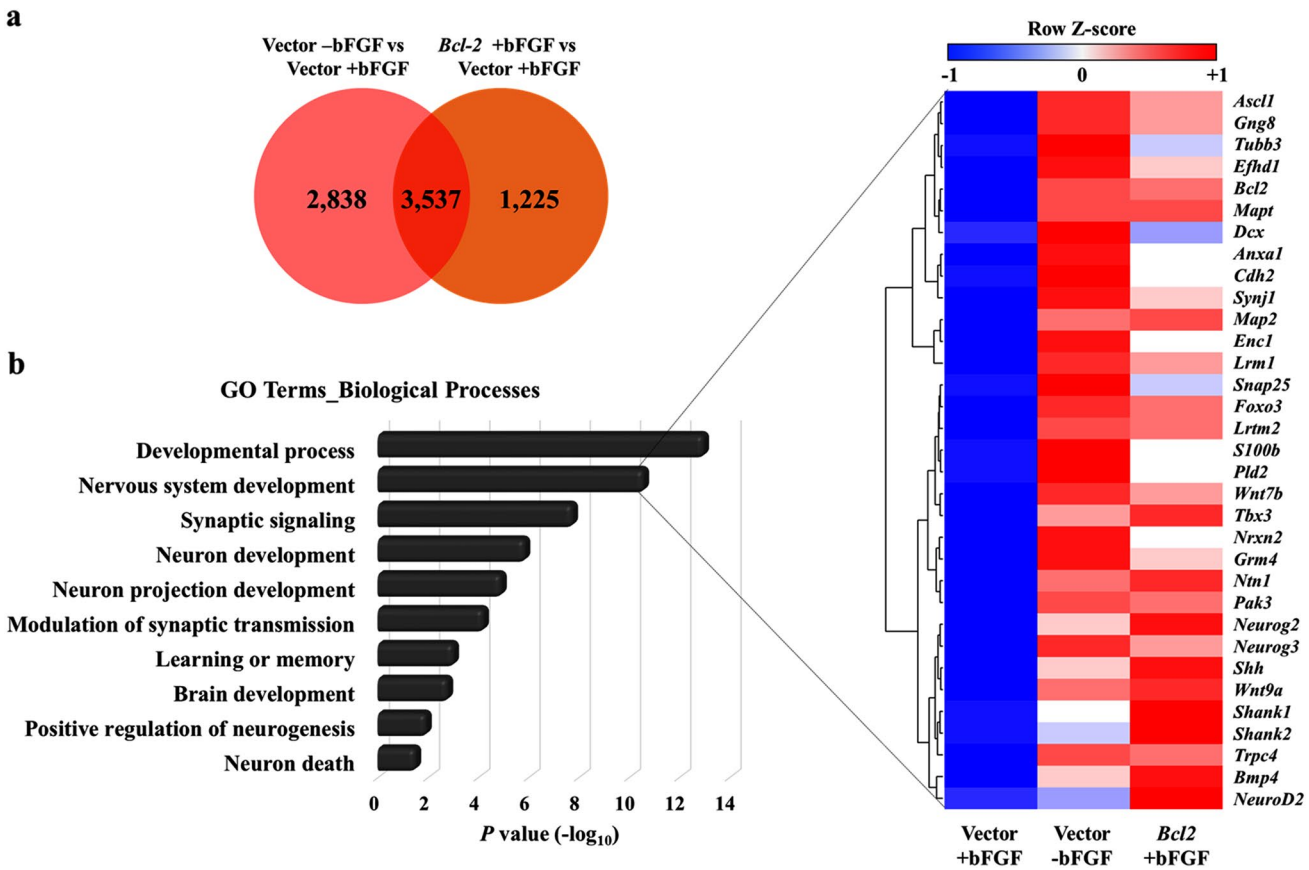

Fig. 2 Microarray analysis of the genes upregulated by *Bcl-2* overexpression in rat NPCs. **a** Whole-genome expression profiles were analyzed using cDNA microarrays of rat NPCs. The number of genes upregulated 1.2-fold by differentiation stimuli or by *Bcl-2* overexpression is shown in the Venn diagram. **b** Upregulated genes were categorized using Gene Ontology (GO) analysis based on the biological processes. The genes corresponding to the nervous system development are expressed in the heat map (right panel). The columns represent the individual groups, and the rows represent each upregulated gene. The relative expression value for each gene is depicted by Z-score, with red indicating high expression and blue indicating low expression

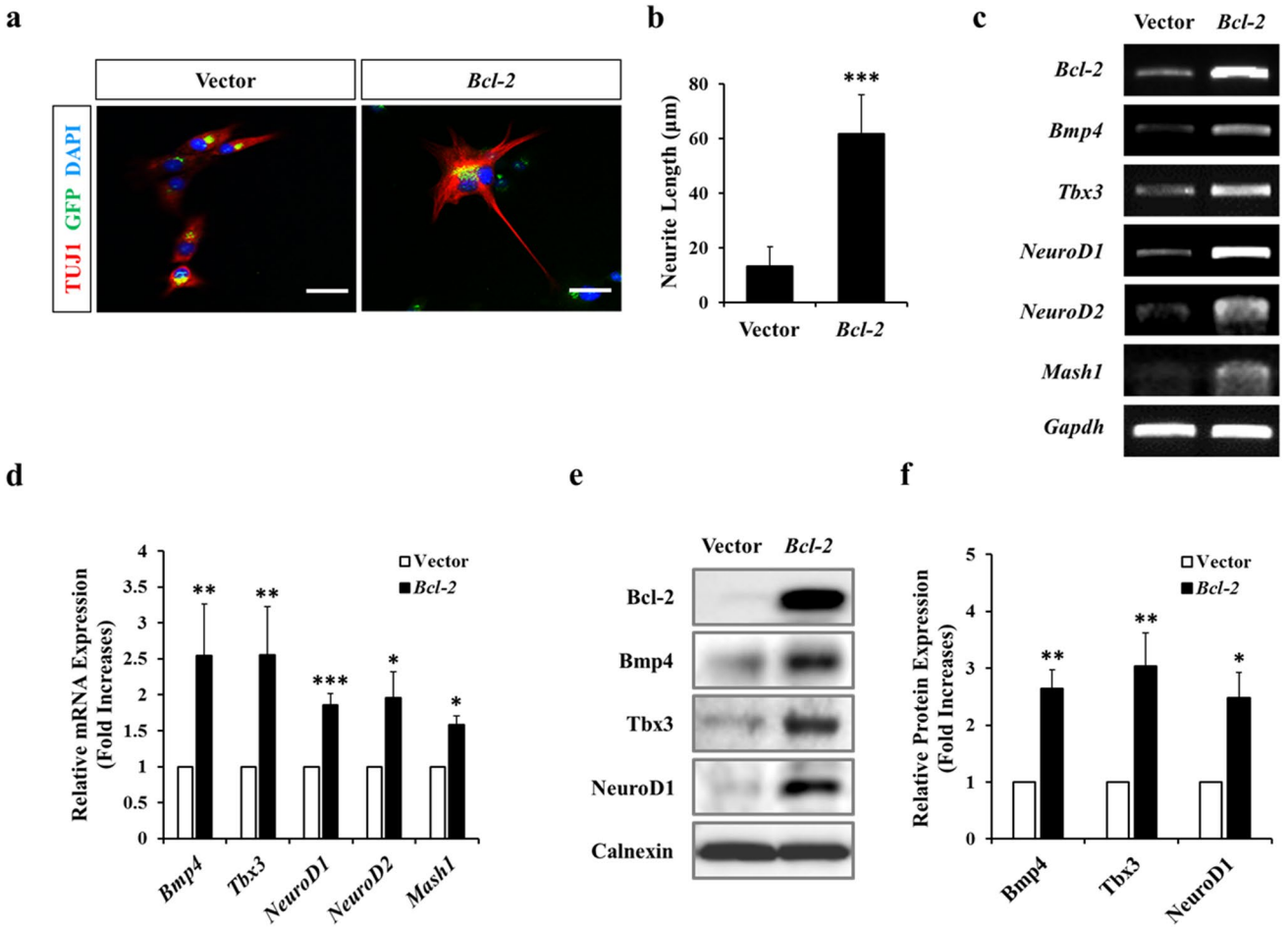

Fig. 3 *Bcl-2* overexpression induces neurite outgrowth as well as expression of several genes. **a** H19-7 cells were infected with MSCV-IRES-EGFP or *rBcl-2*-MSCV-IRES-EGFP using retroviral transduction for 2 days. Immunofluorescence images for TUJ1 and GFP were used to determine neurite outgrowth. Scale bar, 50 μm. **b** The neurite length of TUJ1$^+$ cells was measured from ten randomly selected areas from at least three independent experiments and presented as the mean ± SD. ***$p < 0.001$. **c**, **d** Total RNA was isolated using Trizol reagent, and mRNA levels of *Bcl-2*, *Bmp4*, *Tbx3*, *NeuroD1*, *NeuroD2*, and *Mash1* were determined using RT-PCR (**c**) and real-time RT-PCR (**d**). The results are presented as the mean ± SD of three independent experiments. *$p < 0.05$, **$p < 0.01$, ***$p < 0.001$. **e**, **f** Cells were lysed and analyzed using immunoblotting with anti-Bcl-2, anti-Bmp4, anti-Tbx3, anti-NeuroD1, and anti-Calnexin antibodies. The band intensity was quantified with ImageJ software. The results are presented as the mean density (as a fold increase) ± SD from three independent experiments. *$p < 0.05$, **$p < 0.01$

Bmp4 is Involved in the Process of Neurite Outgrowth Induced by *Bcl-2* Overexpression

Bone morphogenetic proteins (BMPs) are extracellular secretory proteins belonging to the transforming growth factors-β (TGF-β) superfamily and mediate developmental processes, including morphogenesis, proliferation, lineage commitment, differentiation, and apoptosis in the nervous system (Mehler et al. 1997). In particular, Bmp4 is highly expressed in the embryonic cortex of the developing dorsal forebrain (Furuta et al. 1997) and triggers neuronal differentiation of the NPCs in the neocortical ventricular zone (Li et al. 1998; Moon et al. 2009). However, many reports suggest that BMPs and their signaling pathways are involved in the commitment of the astroglial fate during neuronal development in a subclass-specific manner (Mehler et al. 1997; Gross et al. 1996). To investigate the relationship of *Bcl-2* overexpression-induced Bmp4 with other genes, we transfected 100 nM of control or *Bmp4* siRNA into *Bcl-2*-overexpressing H19-7 cells. *Bcl-2*-induced neurite elaboration was significantly repressed by *Bmp4* depletion (Fig. 4a, b). Additionally, the *Bcl-2*-induced expression of Tbx3, NeuroD1, NeuroD2, and Mash1 was strikingly downregulated by *Bmp4* knockdown at both the mRNA (Fig. 4c, d) and protein levels (Fig. 4e, f). These results indicate that Bmp4 participates in Bcl-2-mediated neurite outgrowth by controlling the expression of Tbx3 and neurogenic bHLH transcription factors.

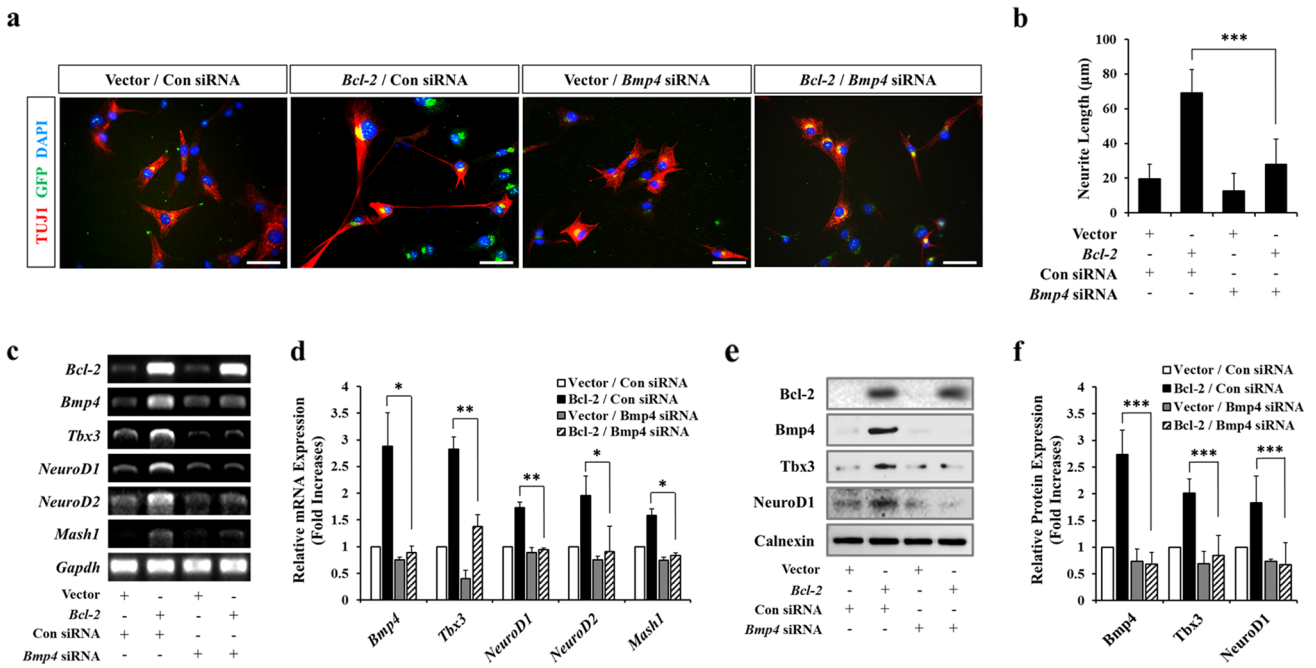

Fig. 4 Effect of *Bmp4* gene depletion in *Bcl-2*-overexpressing H19-7 cells. **a** Cells were infected with MSCV-IRES-EGFP or *rBcl-2*-MSCV-IRES-EGFP using retroviral transduction for 2 days followed by transfection with control or *Bmp4* siRNA. The cells were then immunostained for TUJ1 and GFP. Scale bar, 50 μm. **b** Neurite length was measured. The results are presented as the mean ± SD of three independent experiments. ***$p < 0.001$. **c**, **d** Total RNA was isolated using Trizol reagent, and mRNA levels of *Bcl-2*, *Bmp4*, *Tbx3*, *NeuroD1*, *NeuroD2*, and *Mash1* were determined using RT-PCR (**c**) and real-time RT-PCR (**d**). The results are presented as the mean ± SD of three independent experiments. *$p < 0.05$, **$p < 0.01$. **e**, **f** Cells were lysed, and immunoblotting was performed using anti-Bcl-2, anti-Bmp4, anti-Tbx3, anti-NeuroD1, and anti-Calnexin antibodies. The results are presented as the mean density (as a fold increase) ± SD from three independent experiments. ***$p < 0.001$

The Upregulation of Bmp4 Induced by *Bcl-2* Overexpression is Independent of Canonical Bmp/Smad Pathway

BMPs are secreted extracellularly and bind to their specific receptor leading to the phosphorylation of the Smad1/5/8 protein complex and translocation into the nucleus. The Smad1/5/8 protein complex then acts as a transcription factor and induces the expression of several target genes (Wrana 2013). One of those target genes, Id, represses neuronal differentiation of the NPCs and induces astroglial lineage commitment by preventing DNA binding to neurogenic bHLH transcription factors or by promoting their degradation through ubiquitin-mediated proteolysis (Miyazono and Miyazawa 2002). In addition to these canonical pathways, BMPs also can activate LIMK or the small GTPase Cdc42 instead of phosphorylating Smad. These Smad-independent pathways stimulate cell migration and axon growth (Wrana 2013; Yam and Charron 2013). To examine whether Bcl-2-mediated neurite outgrowth is dependent on Bmp/Smad signaling, we used anti-Bmp4 antibody to neutralize the secreted Bmp4. As shown in Fig. S3, *Bcl-2*-induced upregulation of *Tbx3*, *NeuroD1*, *NeuroD2*, and *Mash1* was reduced by Bmp4 neutralization in a dose-dependent manner. However, neither *Bcl-2* overexpression nor Bmp4 neutralization affected the expression of both *Id1* and *Id2* in H19-7 cells. These results indicate that while Bmp4 induced by *Bcl-2* overexpression can act in an autocrine or paracrine manner after being secreted into the extracellular space, the Smad-dependent canonical pathway is not associated with Bcl-2-mediated neurite formation.

Tbx3 is Also Associated with the Process of Neurite Outgrowth Induced by *Bcl-2* Overexpression

The T-box family of transcription factors, which are characterized by a common DNA binding motif termed as the T-box, are involved in embryonic developmental processes by regulating cell differentiation and migration (Naiche et al. 2005; Papaioannou 2014). In particular, several subfamilies of T-box genes are essential for brain development and their mutations are associated with neurodevelopmental disorders such as autism spectrum disorders (Mihalas and Hevner 2017). Among them, Tbx3 is involved in various signaling pathways related to the pluripotency network and has a critical role in the maintenance of the embryonic stem cells during early cell fate specification (Russell et al. 2015). In order to investigate how Tbx3 impacts other genes during

Bcl-2-mediated neurite outgrowth, we transfected 100 nM of control or *Tbx3* siRNA into *Bcl-2*-overexpressing H19-7 cells. We observed that *Bcl-2*-induced neurite outgrowth was significantly repressed by *Tbx3* depletion (Fig. 5a, b). Moreover, *NeuroD1*, *NeuroD2*, and *Mash1* that were induced by *Bcl-2* overexpression were downregulated by *Tbx3* knockdown, while there was no significant change in the expression of *Bcl-2* and *Bmp4* (Fig. 5c, d). These alterations also coincided with changes in protein levels (Fig. 5e, f). We demonstrated that Tbx3 could mediate the neurite outgrowth by controlling the expression of neurogenic bHLH genes downstream of Bmp4 during Bcl-2-mediated neuronal differentiation.

NeuroD1 is a Key Downstream Regulator of Bcl-2-Mediated Neurite Outgrowth in H19-7 Cells

bHLH proteins possess an HLH domain that enables dimerization and a basic domain for DNA binding (Dennis et al. 2019). bHLH transcription factors are hetero-dimerized with E proteins, which in turn bind to the E-box DNA elements to promote the expression of neurogenic target genes, and their transcriptional activities are inhibited by interaction with the Hes or Id families (Ross et al. 2003). As mentioned previously, we established that Bcl-2 regulated neurite outgrowth by increasing the levels of the proneural bHLH transcription factors, including NeuroD1, NeuroD2, and Mash1, without changing the expression of Id. NeuroD1 is highly accumulated in late development stage of the nervous system and is an essential participant in terminal differentiation, neuronal maturation, and survival (Gao et al. 2009). NeuroD1 also triggers neuronal specification by reprogramming the transcription factor and chromatin landscapes at regulatory elements of neurogenic target genes (Pataskar et al. 2016). To verify the function of NeuroD1, we transfected 100 nM of *NeuroD1* siRNA into *Bcl-2*-overexpressing H19-7 cells. *Bcl-2*-induced neurite elaboration was significantly suppressed by *NeuroD1* knockdown (Fig. 6a, b). However, *NeuroD1* depletion did not influence the expression of other genes (*Bcl-2*, *Bmp4*, *Tbx3*, *NeuroD2*, and *Mash1*) at the mRNA level (Fig. 6c, d). This indicates that NeuroD1 functions independently from other bHLH genes during Bcl-2-mediated neurite outgrowth. Moreover, we found that the protein expression levels of Bcl-2, Bmp4, and Tbx3 did not show any significant changes by the *NeuroD1* knockdown (Fig. 6e, f). In conclusion, we demonstrated that *Bcl-2* overexpression

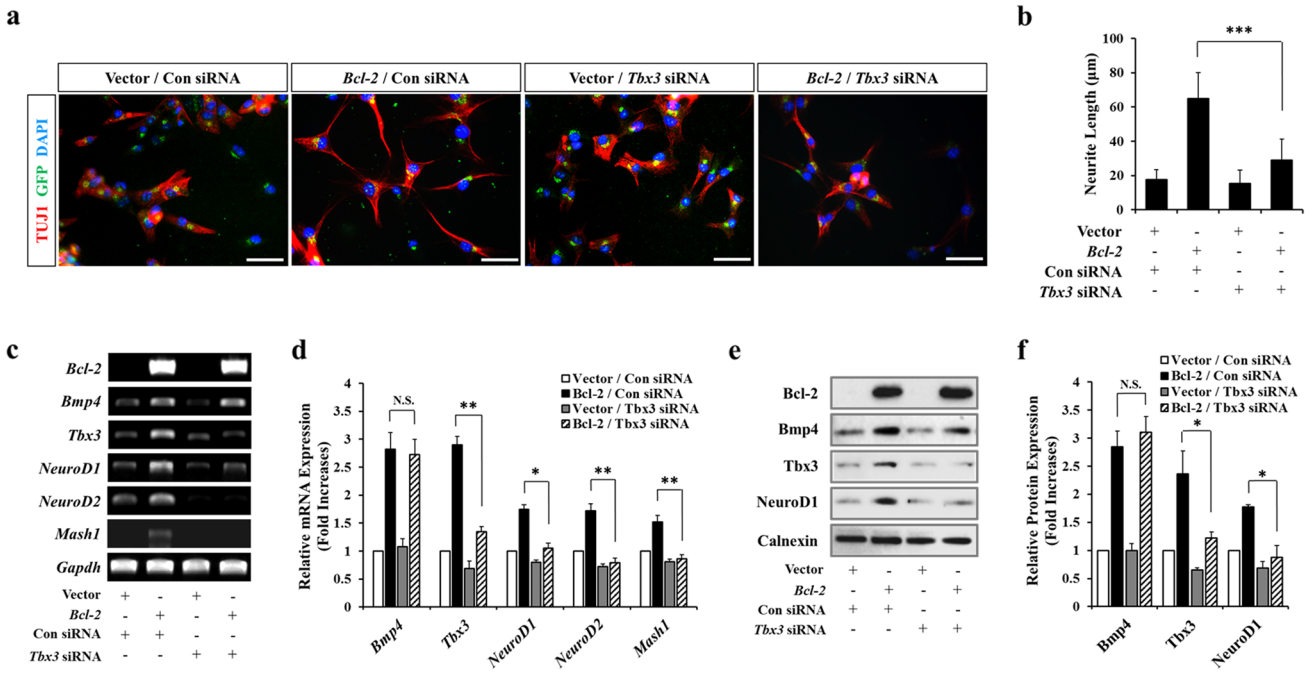

Fig. 5 Effect of *Tbx3* gene depletion in *Bcl-2*-overexpressing H19-7 cells. **a** Cells were infected with MSCV-IRES-EGFP or *rBcl-2*-MSCV-IRES-EGFP via retroviral transduction for 2 days followed by transfection with control or *Tbx3* siRNA. The cells were then immunostained for TUJ1 and GFP. Scale bar, 50 μm. **b** Neurite length was measured. The results are presented as the mean ± SD of three independent experiments. ***$p < 0.001$. **c**, **d** Total RNA was isolated using Trizol reagent, and mRNA levels of *Bcl-2*, *Bmp4*, *Tbx3*, *NeuroD1*, *NeuroD2*, and *Mash1* were determined using RT-PCR (**c**) and real-time RT-PCR (**d**). The results are presented as the mean ± SD of three independent experiments. *$p < 0.05$, **$p < 0.01$. **e**, **f** Cells were lysed, and immunoblotting was performed using anti-Bcl-2, anti-Bmp4, anti-Tbx3, anti-NeuroD1, and anti-Calnexin antibodies. The results are presented as the mean density (as a fold increase) ± SD from three independent experiments. *$p < 0.05$

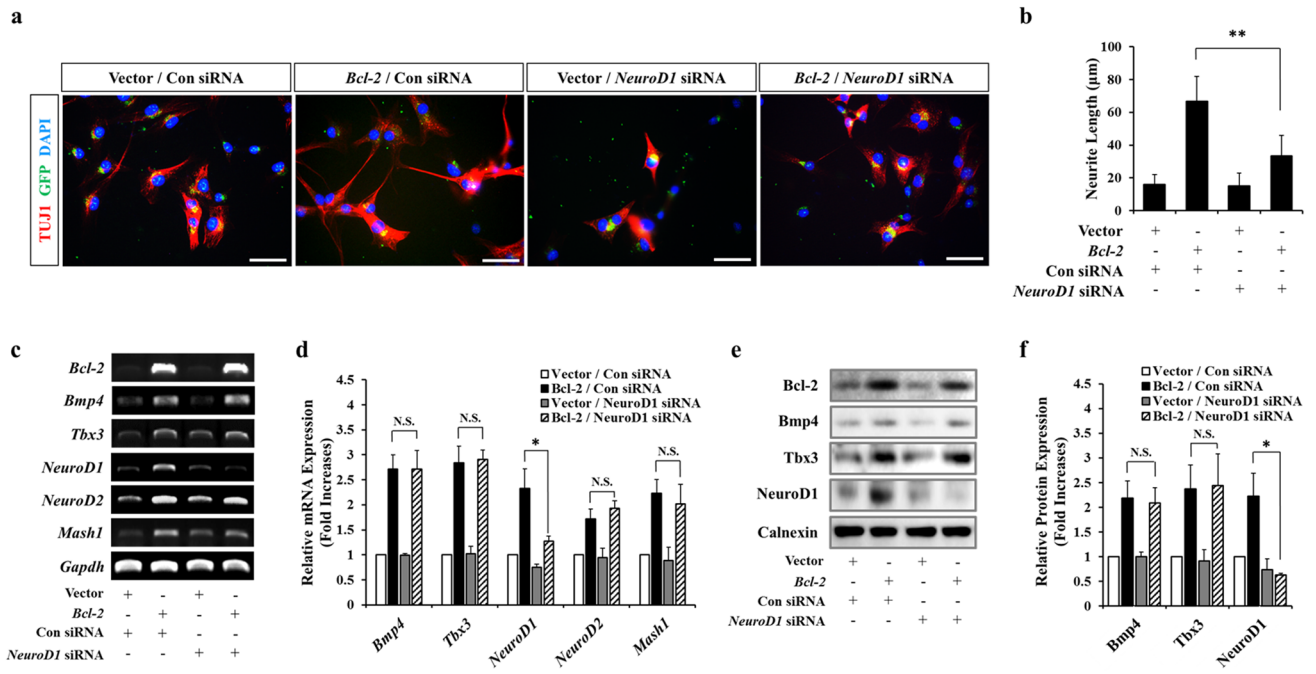

Fig. 6 Effect of *NeuroD1* gene depletion in *Bcl-2*-overexpressing H19-7 cells. **a** Cells were infected with MSCV-IRES-EGFP or *rBcl-2*-MSCV-IRES-EGFP through retroviral transduction for 2 days followed by transfection with control or *NeuroD1* siRNA. The cells were then immunostained for TUJ1 and GFP. Scale bar, 50 μm. **b** Neurite length was measured. The results are presented as the mean ± SD of three independent experiments. $^{**}p < 0.01$. **c**, **d** Total RNA was isolated using Trizol reagent, and mRNA levels of *Bcl-2*, *Bmp4*, *Tbx3*, *NeuroD1*, *NeuroD2*, and *Mash1* were determined using RT-PCR (**c**) and real-time RT-PCR (**d**). The results are presented as the mean ± SD of three independent experiments. $^{*}p < 0.05$. **e**, **f** Cells were lysed, and immunoblotting was performed using anti-Bcl-2, anti-Bmp4, anti-Tbx3, anti-NeuroD1, and anti-Calnexin antibodies. The results are presented as the mean density (as a fold increase) ± SD from three independent experiments. $^{*}p < 0.05$

promotes neurite formation via the Bmp4/Tbx3/NeuroD1 pathway in H19-7 cells.

Discussion

Multipotent neural stem cells can give rise to all types of neural cells through asymmetric cell division, including neurons, astrocytes, and oligodendrocytes in the mammalian nervous system (Gage 2000; Paridaen and Huttner 2014). They are spatiotemporally controlled by intrinsic or extrinsic factors found in the neural stem cell niche (Paridaen and Huttner 2014). In particular, bFGF is a necessary stem cell mitogen required for proliferation and neurogenesis during the development of the nervous system (Raballo et al. 2000). It interacts with receptor tyrosine kinase FGFRs (FGF receptors) on the cell surface and triggers various cellular processes by activating downstream molecules including Ras, phospholipase C, and phosphoinositide 3-kinase via tyrosine phosphorylation of the adaptor protein FRS2 (FGF receptor substrate 2) (Schlessinger 2004). We previously reported that PLD1 plays an important role in bFGF signaling involved in neuronal differentiation in rat hippocampal progenitor cells. PLD1 is activated by Src and Ras during bFGF-induced neurite outgrowth and regulates neurotrophin-3 expression through the RhoA/ROCK/JNK/Elk1 pathway in H19-7 cells (Oh et al. 2007; Choi et al. 2012). Furthermore, PLD1 upregulates Bcl-2 expression through the PLA2/Cox2/EP4/PKA/p38MAPK/CREB cascade in rat NPCs and through the JNK/STAT3 pathway in H19-7 cells during neuronal differentiation (Park et al. 2014; Yoon et al. 2012). This indicates that PLD1-mediated Bcl-2 expression is required in bFGF signaling for neuronal fate determination of NPCs. However, the mechanism by which Bcl-2 influences neuronal differentiation is not fully understood.

Bcl-2 is generally regarded as an anti-apoptotic protein that prevents the cytosolic release of apoptogenic factors, including cytochrome *c*, in the mitochondrial outer membrane (Adams and Cory 1998; Pan et al. 2014, 2015). Many previous reports have shown the neuroprotective effects of Bcl-2 against environmental insults such as ischemia (Martinou et al. 1994). Moreover, the interaction of Bcl-2 with calcineurin can inhibit Ca^{2+} release by suppressing IP_3R (inositol 1,4,5-triphosphate receptor) through the phosphatase cascade of DARPP-32 (dopamine and cAMP-regulated phosphoprotein-32)/PP1α (protein phosphatase 1

alpha) on the endoplasmic reticulum (ER) (Tang et al. 2003; Erin et al. 2003). These mechanisms may also be involved in neuropsychiatric disorders. Bcl-2 rs956572 polymorphism has been found to be associated with dysfunction of intracellular Ca^{2+} homeostasis and the cortical glutamatergic system in the pathophysiology of type I bipolar disorder (Uemura et al. 2011; Soeiro-de-Souza et al. 2013). Moreover, mood-stabilizing agents, such as lithium and valproate, increase Bcl-2 expression in the rat CNS (Chen et al. 1999). Bcl-2 family proteins are involved in the development of resistance against therapy-induced apoptosis during the treatment of several types of brain cancers such as malignant glioblastoma (Strik et al. 1999; Fels et al. 2000). Taken together, this strongly indicates the possibility that Bcl-2 can be a potential therapeutic target. Recently, the use of the BH3-mimetic drug Venetoclax (ABT-199) is on the rise as a Bcl-2 inhibitor in various fields including clinical lymphoma therapy (King et al. 2017). However, it still needs to be confirmed whether this drug can also be used to treat brain cancer. In addition, studies using various cancer models have suggested that Bcl-2 expression is intimately regulated by PLD1, indicating that targeting PLD1 might have robust anticancer effects via the inhibition of Bcl-2 function (Cho et al. 2008). The small-molecule PLD1 inhibitor FIPI shows remarkable preclinical efficacy for the treatment of colorectal cancer (Kang et al. 2015), and the peptide drug TVTSP, a PLD1-specific inhibitor, was recently verified as an efficient therapeutic agent for several types of cancer and other inflammatory conditions (Cho et al. 2011; Lee et al. 2018). Therefore, detailed research needs to be done in the future to evaluate if these drugs can also be considered as potential therapeutics for several brain disorders.

Apart from its neuroprotective function, Bcl-2 mediates neurogenesis for the developing CNS and the regenerating adult nervous system (Michaelidis et al. 1996; Zhang et al. 1996; Hilton et al. 1997; Chen et al. 1997). However, it is unclear whether Bcl-2 exerts its neuroprotective effect by merely providing sufficient time for neurogenesis of NPCs by protecting them from cell death. Loss of *Bcl-2* function represses neurite elaboration in response to differentiation stimuli, and inversely, gain of *Bcl-2* function enhanced neurite outgrowth (Fig. 1), indicating that Bcl-2 is strongly involved in the neuronal differentiation process. Next, we sought to determine how Bcl-2 impacts neurite outgrowth. According to previous reports, *Bcl-2* overexpression increases synaptosomal-associated protein 25 (SNAP-25) in a dopaminergic neuronal cell line (Oh et al. 1996). Moreover, Suzuki and Tsutomi (1998) suggested that Bcl-2 controls neuronal differentiation by accelerating polymerization of neurofilament chains, and Chang et al. (2007) reported that *Bcl-*X_L overexpression induces proneural bHLH genes (*Ngn1*, *NeuroD1*, and *Mash1*) and suppresses anti-neuronal bHLH genes (*Hes1/5* and *Id1/2/3*) without changing the expression of the Notch signaling genes. Therefore, we analyzed the whole-genome expression profiles of rat NPCs to compare the genes that were altered by differentiation stimuli and the genes affected by *Bcl-2* overexpression. Similar to the differentiated control group, *Bcl-2* overexpression increased many neurogenic marker genes (Fig. 2b). In particular, proneural bHLH genes, including *NeuroD2*, *Neurog2*, and *Mash1*, were upregulated. When *Bcl-2* was overexpressed in H19-7 cells, neurite length was significantly increased, and *NeuroD1*, *NeuroD2*, and *Mash1* were also upregulated (Fig. 3). However, the expression of *Neurog1* and *Neurog2* was not affected (data not shown). These results imply that *Bcl-2* overexpression has a direct impact on the neuronal differentiation through upregulation of neurogenic bHLH genes. Additionally, we found that *Bcl-2* overexpression significantly increased Bmp4 and Tbx3 expression, indicating that Bmp4, Tbx3, and several bHLH transcription factors are included in Bcl-2-mediated neurite outgrowth.

To investigate the hierarchy of these molecules, we selectively depleted *Bmp4*, *Tbx3*, or *NeuroD1* in *Bcl-2*-overexpressing H19-7 cells. When *Bmp4* was depleted, Bcl-2-mediated neurite formation was significantly repressed, and Tbx3 and NeuroD1 were downregulated (Fig. 4), indicating that Bmp4 is required for Bcl-2-mediated neurite outgrowth by regulating Tbx3 and NeuroD1. Bmp4 induces neuronal differentiation in the neocortical ventricular zone (Li et al. 1998; Moon et al. 2009). However, many reports suggest that BMPs might induce astroglial fate specification (Mehler et al. 1997; Gross et al. 1996). It is thought that this discrepancy occurs due to the dependency of Bmp4 on Smad. Extracellularly secreted Bmp4 activates Smad1/5/8 protein by binding to BMP receptors on the cell surface, which facilitates Smad1/5/8 to act as a transcriptional regulator and induce the expression of the target genes including Id (Wrana 2013; Miyazono and Miyazawa 2002). Conversely, Bmp4 can induce axon growth by activating LIMK or the small GTPase Cdc42 without Smad phosphorylation (Wrana 2013; Yam and Charron 2013). In this study, Bmp4 neutralization downregulated its downstream genes (*Tbx3*, *NeuroD1*, *NeuroD2*, and *Mash1*) without affecting the expression of *Id1* and *Id2* (Fig. S3). In addition, Smad1 was not phosphorylated by *Bcl-2* overexpression (data not shown). These results indicate that although the Smad-dependent canonical pathway might not be associated with Bcl-2-mediated neurite formation, Bmp4 functions in an autocrine or paracrine manner after being secreted into the extracellular space. Bcl-2 also increases stroke-induced striatal neurogenesis in adult brains by modulating Bmp4 function via activation of β-catenin signaling (Lei et al. 2012). The expression of Bmp4 induced by *Bcl-2* overexpression has been thought to be mediated by Wnt/β-catenin signaling. We also found that Tbx3 acts downstream of Bmp4 and controls neurite

outgrowth by increasing the expression of the neurogenic bHLH genes during Bcl-2-mediated neuronal differentiation (Fig. 5). Bmp4 has been shown to induce Tbx3 expression in the pathophysiology of glomerular diseases (Wensing and Campos 2014), and β-catenin reinforces the pluripotency by activating Oct-4 via a TCF-independent mechanism, which induces the expression of Tbx3 as a Oct-4 target gene (Kelly et al. 2011). Moreover, Tbx3 mediates TGF-β1-induced antiproliferative and pro-migratory effects in breast epithelial cells by repressing Tbx2 transcription, which allows for the derepression of p21 and a G1 cell cycle arrest (Li et al. 2013). Finally, while Bcl-2-mediated neurite outgrowth was significantly suppressed by *NeuroD1* knockdown, the expression of other genes was not altered (Fig. 6). This indicates that NeuroD1 functions independently of other bHLH genes during Bcl-2-mediated neurite outgrowth and that *Bcl-2* overexpression promotes neurite elaboration via the Bmp4/Tbx3/NeuroD1 pathway. Taken together, this study shows that Bcl-2 may have a direct role in neuronal differentiation in addition to its well-known anti-apoptotic function in response to environmental insults.

Conclusions

We demonstrated that *Bcl-2* overexpression induces neurite outgrowth through the Bmp4/Tbx3/NeuroD1 cascade, thereby contributing to understanding of the non-apoptotic function of Bcl-2 during neuronal differentiation.

Acknowledgements This work was supported by a National Research Foundation of Korea (NRF) Grant funded by the Korean government (MSIP) (NRF-2016R1A2B4015358) and partly supported by the Basic Science Research Program through the National Research Foundation of Korea (NRF) funded by the Ministry of Education (NRF-2013R1A1A2061420). In addition, this research was supported by a grant of the Korea Health Technology R&D Project through the Korea Health Industry Development Institute (KHIDI), funded by the Ministry of Health & Welfare, Republic of Korea (Grant Number: HI19C0611), and supported by the research fund of Hanyang University (HY-2019).

Author Contributions YY Lee conceptualized and designed of the study, collected and assembled the data, analyzed and interpreted the results, and wrote the manuscript. H-J Choi conceptualized and designed the study and provided financial support. SY Lee analyzed the microarray data and performed some of the experiments. S-Y Park analyzed and interpreted the results. M-J Kang conducted some of the experiments. J Han analyzed the microarray data. J-S Han conceptualized and designed the study, analyzed and interpreted the data, wrote the manuscript, and provided financial support. All authors read and approved the final manuscript.

Compliance with Ethical Standards

Conflict of interest The authors declare that they have no conflicts of interest.

References

Abedohmae S, Harada N, Yamada K, Tanaka R (1993) Bcl-2 gene highly expressed during neurogenesis in the central nervous system. Biochem Biophys Res Commun 191:915–921. https://doi.org/10.1006/bbrc.1993.1304

Adams JM, Cory S (1998) The Bcl-2 protein family: arbiters of cell survival. Science 281:1322–1326. https://doi.org/10.1126/science.281.5381.1322

Allsopp TE, Wyatt S, Paterson HF, Davies AM (1993) The proto-oncogene bcl-2 can selectively rescue neurotrophic factor-dependent neurons from apoptosis. Cell 73:295–307. https://doi.org/10.1016/0092-8674(93)90230-N

Chang MY et al (2007) Bcl-XL/Bax proteins direct the fate of embryonic cortical precursor cells. Mol Cell Biol 27:4293–4305. https://doi.org/10.1128/MCB.00031-07

Chen DF, Schneider GE, Martinou JC, Tonegawa S (1997) Bcl-2 promotes regeneration of severed axons in mammalian CNS. Nature 385:434–439. https://doi.org/10.1038/385434a0

Chen G, Zeng WZ, Yuan PX, Huang LD, Jiang YM, Zhao ZH, Manji HK (1999) The mood-stabilizing agents lithium and valproate robustly increase the levels of the neuroprotective protein bcl-2 in the CNS. J Neurochem 72:879–882. https://doi.org/10.1046/j.1471-4159.1999.720879.x

Cho JH et al (2008) Overexpression of phospholipase D suppresses taxotere-induced cell death in stomach cancer cells. Biochim Biophys Acta 1783:912–923. https://doi.org/10.1016/j.bbamcr.2007.11.019

Cho JH et al (2011) The TSP motif in AP180 inhibits phospholipase D1 activity resulting in increased efficacy of anticancer drug via its direct binding to carboxyl terminal of phospholipase D1. Cancer Lett 302:144–154. https://doi.org/10.1016/j.canlet.2011.01.005

Choi HJ, Chang BJ, Han JS (2012) Phospholipase D1 is an important regulator of bFGF-induced neurotrophin-3 expression and neurite outgrowth in H19-7 cells. Mol Neurobiol 45:507–519. https://doi.org/10.1007/s12035-012-8268-7

Dennis DJ, Han S, Schuurmans C (2019) bHLH transcription factors in neural development, disease, and reprogramming. Brain Res 1705:48–65. https://doi.org/10.1016/j.brainres.2018.03.013

Erin N, Bronson SK, Billingsley ML (2003) Calcium-dependent interaction of calcineurin with bcl-2 in neuronal tissue. Neuroscience 117:541–555. https://doi.org/10.1016/s0306-4522(02)00933-8

Fels C et al (2000) Bcl-2 expression in higher-grade human glioma: a clinical and experimental study. J Neurooncol 48:207–216. https://doi.org/10.1023/A:1006484801654

Furuta Y, Piston DW, Hogan BL (1997) Bone morphogenetic proteins (BMPs) as regulators of dorsal forebrain development. Development 124:2203–2212

Gage FH (2000) Mammalian neural stem cells. Science 287:1433–1438. https://doi.org/10.1126/science.287.5457.1433

Gao Z et al (2009) Neurod1 is essential for the survival and maturation of adult-born neurons. Nat Neurosci 12:1090–1092. https://doi.org/10.1038/nn.2385

Gross RE, Mehler MF, Mabie PC, Zang Z, Santschi L, Kessler JA (1996) Bone morphogenetic proteins promote astroglial lineage commitment by mammalian subventricular zone progenitor cells. Neuron 17:595–606. https://doi.org/10.1016/S0896-6273(00)80193-2

Hanada M, Krajewski S, Tanaka S, Cazals-Hatem D, Spengler BA, Ross RA, Biedler JLR, Reed JC (1993) Regulation of Bcl-2 oncoprotein levels with differentiation of human neuroblastoma cells. Cancer Res 53:4978–4986

Hilton M, Middleton G, Davies AM (1997) Bcl-2 influences axonal growth rate in embryonic sensory neurons. Curr Biol 7:798–800. https://doi.org/10.1016/S0960-9822(06)00339-3

Hockenbery D, Nuñez G, Milliman C, Schreiber RD, Korsmeyer SJ (1990) Bcl-2 is an inner mitochondrial membrane protein that blocks programmed cell death. Nature 348:334–336. https://doi.org/10.1038/348334a0

Hockenbery DM, Zutter M, Hickey W, Nahm M, Korsmeyer SJ (1991) BCL2 protein is topographically restricted in tissues characterized by apoptotic cell death. Proc Natl Acad Sci USA 88:6961–6965. https://doi.org/10.1073/pnas.88.16.6961

Kang DW, Choi CY, Cho YH, Tian H, Di Paolo G, Choi KY, Min Do S (2015) Targeting phospholipase D1 attenuates intestinal tumorigenesis by controlling beta-catenin signaling in cancer-initiating cells. J Exp Med 212:1219–1237. https://doi.org/10.1084/jem.20141254

Kelly KF, Ng DY, Jayakumaran G, Wood GA, Koide H, Doble BW (2011) β-catenin enhances Oct-4 activity and reinforces pluripotency through a TCF-independent mechanism. Cell Stem Cell 8:214–227. https://doi.org/10.1016/j.stem.2010.12.010

King AC, Peterson TJ, Horvat TZ, Rodriguez M, Tang LA (2017) Venetoclax: a first-in-class oral BCL-2 inhibitor for the management of lymphoid malignancies. Ann Pharmacother 51:410–416. https://doi.org/10.1177/1060028016685803

Lee YY, Lee SY, Park SY, Choi HJ, Kim EG, Han JS (2018) Therapeutic potential of a phospholipase D1 inhibitory peptide fused with a cell-penetrating peptide as a novel anti-asthmatic drug in a *Der f* 2-induced airway inflammation model. Exp Mol Med 50:55. https://doi.org/10.1038/s12276-018-0083-4

Lei ZN, Liu F, Zhang LM, Huang YL, Sun FY (2012) Bcl-2 increases stroke-induced striatal neurogenesis in adult brains by inhibiting BMP-4 function via activation of beta-catenin signaling. Neurochem Int 61:34–42. https://doi.org/10.1016/j.neuint.2012.04.004

Li W, Cogswell CA, LoTurco JJ (1998) Neuronal differentiation of precursors in the neocortical ventricular zone is triggered by BMP. J Neurosci 18:8853–8862. https://doi.org/10.1523/JNEUROSCI.18-21-08853.1998

Li J, Weinberg MS, Zerbini L, Prince S (2013) The oncogenic TBX3 is a downstream target and mediator of the TGF-β1 signaling pathway. Mol Biol Cell 24:3569–3576. https://doi.org/10.1091/mbc.E13-05-0273

Martinou JC et al (1994) Overexpression of BCL-2 in transgenic mice protects neurons from naturally occurring cell death and experimental ischemia. Neuron 13:1017–1030. https://doi.org/10.1016/0896-6273(94)90266-6

Mehler MF, Mabie PC, Zhang D, Kessler JA (1997) Bone morphogenetic proteins in the nervous system. Trends Neurosci 20:309–317. https://doi.org/10.1016/S0166-2236(96)01046-6

Merry DE, Veis DJ, Hickey WF, Korsmeyer SJ (1994) Bcl-2 protein expression is widespread in the developing nervous system and retained in the adult PNS. Development 120:301–311

Michaelidis TM, Sendtner M, Cooper JD, Airaksinen MS, Holtmann B, Meyer M, Thoenen H (1996) Inactivation of bcl-2 results in progressive degeneration of motoneurons, sympathetic and sensory neurons during early postnatal development. Neuron 17:75–89. https://doi.org/10.1016/S0896-6273(00)80282-2

Mihalas AB, Hevner RF (2017) Control of neuronal development by T-Box genes in the brain. Curr Top Dev Biol 122:279–312. https://doi.org/10.1016/bs.ctdb.2016.08.001

Miyazono K, Miyazawa K (2002) Id: a target of BMP signaling. Sci STKE. https://doi.org/10.1126/stke.2002.151.pe40

Moon BS, Yoon JY, Kim MY, Lee SH, Choi T, Choi KY (2009) Bone morphogenetic protein 4 stimulates neuronal differentiation of neuronal stem cells through the ERK pathway. Exp Mol Med 41:116–125. https://doi.org/10.3858/emm.2009.41.2.014

Naiche LA, Harrelson Z, Kelly RG, Papaioannou VE (2005) T-box genes in vertebrate development. Annu Rev Genet 39:219–239. https://doi.org/10.1146/annurev.genet.39.073003.105925

Oh YJ, Swarzenski BC, O'Malley KL (1996) Overexpression of Bcl-2 in a murine dopaminergic neuronal cell line leads to neurite outgrowth. Neurosci Lett 202:161–164. https://doi.org/10.1016/0304-3940(95)12235-4

Oh DY, Park SY, Cho JH, Lee KS, Min Do S, Han JC (2007) Phospholipase D1 activation through Src and Ras is involved in basic fibroblast growth factor-induced neurite outgrowth of H19-7 cells. J Cell Biochem 101:221–234. https://doi.org/10.1002/jcb.21166

Pan B et al (2014) C-Abl tyrosine kinase mediates neurotoxic prion peptide-induced neuronal apoptosis via regulating mitochondrial homeostasis. Mol Neurobiol 49:1102–1116. https://doi.org/10.1007/s12035-014-8646-4

Pan Y et al (2015) STI571 protects neuronal cells from neurotoxic prion protein fragment-induced apoptosis. Neuropharmacology 93:191–198. https://doi.org/10.1016/j.neuropharm.2015.01.029

Pan B, Zhang H, Cui T, Wang X (2017) TFEB activation protects against cardiac proteotoxicity via increasing autophagic flux. J Mol Cell Cardiol 113:51–62. https://doi.org/10.1016/j.yjmcc.2017.10.003

Papaioannou VE (2014) The T-box gene family: emerging roles in development, stem cells and cancer. Development 141:3819–3833. https://doi.org/10.1242/dev.104471

Paridaen JT, Huttner WB (2014) Neurogenesis during development of the vertebrate central nervous system. EMBO Rep 15:351–364. https://doi.org/10.1002/embr.201438447

Park SY, Han JS (2018) Phospholipase D1 signaling: essential roles in neural stem cell differentiation. J Mol Neurosci 64:333–340. https://doi.org/10.1007/s12031-018-1042-1

Park SY, Ma W, Yoon SN, Kang MJ, Han JS (2014) Phospholipase D1 increases Bcl-2 expression during neuronal differentiation of rat neural stem cells. Mol Neurobiol 51:1089–1102. https://doi.org/10.1007/s12035-014-8773-y

Pataskar A, Jung J, Smialowski P, Noack F, Calegari F, Straub T, Tiwari VK (2016) NeuroD1 reprograms chromatin and transcription factor landscapes to induce the neuronal program. EMBO J 35:24–45. https://doi.org/10.15252/embj.201591206

Pattingre S et al (2005) Bcl-2 antiapoptotic proteins inhibit Beclin 1-dependent autophagy. Cell 122:927–939. https://doi.org/10.1016/j.cell.2005.07.002

Pegoraro L et al (1984) A 14;18 and an 8;14 chromosome translocation in a cell line derived from an acute B-cell leukemia. Proc Natl Acad Sci USA 81:7166–7170. https://doi.org/10.1073/pnas.81.22.7166

Raballo R, Rhee J, Lyn-Cook R, Leckman JF, Schwartz ML, Vaccarino FM (2000) Basic fibroblast growth factor (Fgf2) is necessary for cell proliferation and neurogenesis in the developing cerebral cortex. J Neurosci 20:5012–5023. https://doi.org/10.1523/JNEUROSCI.20-13-05012.2000

Ross SE, Greenberg ME, Stiles CD (2003) Basic helix-loop-helix factors in cortical development. Neuron 39:13–25. https://doi.org/10.1016/s0896-6273(03)00365-9

Russell R et al (2015) A dynamic role of TBX3 in the pluripotency circuitry. Stem Cell Rep 5:1155–1170. https://doi.org/10.1016/j.stemcr.2015.11.003

Sato N, Hotta K, Waguri S, Nitatori T, Tohyama K, Tsujimoto Y, Uchiyama Y (1994) Neuronal differentiation of PC12 cells as a result of prevention of cell death by bcl-2. J Neurobiol 25:1227–1234. https://doi.org/10.1002/neu.480251005

Schlessinger J (2004) Common and distinct elements in cellular signaling via EGF and FGF receptors. Science 306:1506–1507. https://doi.org/10.1126/science.1105396

Soeiro-de-Souza MG et al (2013) Bcl-2 rs956572 polymorphism is associated with increased anterior cingulate cortical glutamate in euthymic bipolar I disorder. Neuropsychopharmacology 38:468–475. https://doi.org/10.1038/npp.2012.203

Strik H et al (1999) BCL-2 family protein expression in initial and recurrent glioblastomas: modulation by radiochemotherapy. J Neurol Neurosurg Pshychiatry 67:763–768. https://doi.org/10.1136/jnnp.67.6.763

Suzuki A, Tsutomi Y (1998) Bcl-2 accelerates the neuronal differentiation: new evidence approaching to the biofunction of Bcl-2 in the neuronal system. Brain Res 801:59–66. https://doi.org/10.1016/S0006-8993(98)00523-X

Tang TS, Tu H, Wang Z, Bezprozvanny I (2003) Modulation of type 1 inositol (1,4,5)-trisphosphate receptor function by protein kinase a and protein phosphatase 1alpha. J Neurosci 23:403–415. https://doi.org/10.1523/JNEUROSCI.23-02-00403.2003

Uemura T, Green M, Corson TW, Perova T, Li PP, Warsh JJ (2011) Bcl-2 SNP rs956572 associates with disrupted intracellular calcium homeostasis in bipolar I disorder. Bipolar Disord 13:41–51. https://doi.org/10.1111/j.1399-5618.2011.00897.x

Wensing LA, Campos AH (2014) TBX3, a downstream target of TGF-β1, inhibits mesangial cell apoptosis. Exp Cell Res 328:340–350. https://doi.org/10.1016/j.yexcr.2014.08.022

Wrana JL (2013) Signaling by the TGFbeta superfamily. Cold Spring Harb Perspect Biol 5:a011197. https://doi.org/10.1101/cshperspect.a011197

Yam PT, Charron F (2013) Signaling mechanisms of non-conventional axon guidance cues: the Shh, BMP and Wnt morphogens. Curr Opin Neurobiol 23:965–973. https://doi.org/10.1016/j.conb.2013.09.002

Yoon SN, Kim KS, Cho JH, Ma W, Choi HJ, Kwon SJ, Han JS (2012) Phospholipase D1 mediates bFGF-induced Bcl-2 expression leading to neurite outgrowth in H19-7 cells. Biochem J 441:407–416. https://doi.org/10.1042/BJ20110302

Zhang KZ, Westberg JA, Hölttä E, Andersson LC (1996) BCL2 regulates neural differentiation. Proc Natl Acad Sci USA 93:4504–4508. https://doi.org/10.1073/pnas.93.9.4504

Zhang H, Pan B, Wu P, Parajuli N, Rekhter MD, Goldberg AL, Wang X (2019) PDE1 inhibition facilitates proteasomal degradation of misfolded proteins and protects against cardiac proteinopathy. Sci Adv 5:5870. https://doi.org/10.1126/sciadv.aaw5870